1521-0103/375/1/1–9$35.00
THE JOURNAL OF PHARMACOLOGY AND EXPERIMENTAL THERAPEUTICS

https://doi.org/10.1124/jpet.120.265942
J Pharmacol Exp Ther 375:1–9, October 2020

Mirtazapine, an α2 Antagonist-Type Antidepressant, Reverses Pain and Lack of Morphine Analgesia in Fibromyalgia-Like Mouse Models[S]

Hiroyuki Neyama,[1] Naoki Dozono,[2] Hitoshi Uchida,[3] and Hiroshi Ueda[2]

Department of Pharmacology and Therapeutic Innovation, Nagasaki University Graduate School of Biomedical Sciences, Nagasaki, Japan

Received February 25, 2020; accepted July 13, 2020

ABSTRACT

Treatment of fibromyalgia is an unmet medical need; however, its pathogenesis is still poorly understood. In a series of studies, we have demonstrated that some pharmacological treatments reverse generalized chronic pain but do not affect the lack of morphine analgesia in the intermittent cold stress (ICS)–induced fibromyalgia-like pain model in mice. Here we report that repeated intraperitoneal treatments with mirtazapine, which is presumed to disinhibit 5-hydroxytriptamine (5-HT) release and activate 5-HT1 receptor through mechanisms of blocking presynaptic adrenergic α2 and postsynaptic 5-HT2 and 5-HT3 receptors, completely reversed the chronic pain for more than 4 to 5 days after the cessation of treatments. The repeated mirtazapine treatments also recovered the morphine analgesia after the return of nociceptive threshold to the normal level. The microinjection of small interfering RNA (siRNA) adrenergic α2a receptor (ADRA2A) into the habenula, which showed a selective upregulation of α2 receptor gene expression after ICS, reversed the hyperalgesia but did not recover the morphine analgesia. However, both reversal of hyperalgesia and recovery of morphine analgesia were observed when siRNA ADRA2A was administered intracerebroventricularly. As the habenular is reported to be involved in the emotion/reward-related pain and hypoalgesia, these results suggest that mirtazapine could attenuate pain and/or augment hypoalgesia by blocking the habenular α2 receptor after ICS. The recovery of morphine analgesia in the ICS model, on the other hand, seems to be mediated through a blockade of α2 receptor in unidentified brain regions.

SIGNIFICANCE STATEMENT

This study reports possible mechanisms underlying the complete reversal of hyperalgesia and recovery of morphine analgesia by mirtazapine, a unique antidepressant with adrenergic α2 and serotonergic receptor antagonist properties, in a type of intermittently repeated stress (ICS)–induced fibromyalgia-like pain model. Habenula, a brain region which is related to the control of emotional pain, was found to play key roles in the antihyperalgesia, whereas other brain regions appeared to be involved in the recovery of morphine analgesia in the ICS model.

Introduction

Since animal models of neuropathic pain were developed (Bennett and Xie, 1988; Ossipov and Porreca, 2013), much effort has been devoted to clarifying the underlying mechanisms toward the end of discovering novel treatments for neuropathic pain by using physiologic, anatomic (Basbaum et al., 2009; Devor, 2013), and molecular biologic techniques (Ueda, 2006, 2008; Costigan et al., 2009; Kuner, 2010; Hill, 2013). Compared with the studies of neuropathic pain, the basic research on chronic widespread pain syndromes, such as fibromyalgia (FM), which is lacking obvious etiology, has been much less advanced, despite 2% of the population suffering from FM (Russell, 2013; Clauw, 2014). As patients with FM are reported to have shown diverse and inconsistent biochemical changes (Russell, 2005), the current information does not seem to be enough for the use in diagnosis and treatment of patients with FM. Therefore, basic studies, including pathophysiology and pharmacotherapy using animal models, for FM-like syndromes (Sluka and Clauw, 2016) are indispensable.

The pioneering works by Levine and colleagues and other group have demonstrated that vagotomized animals show widespread pain (Khasar et al., 1998a,b; Chen et al., 2008). Regarding pharmacological aspects, there is a report that vagotomy-induced hyperalgesia is sensitive to antidepressants, gabapentinoids, and

This work was supported in part by Grants-in-Aid for the Platform for Drug Discovery, Informatics, and Structural Life Science [16am0101012j0005 to H.U.] from the Japan Agency for Medical Research and Development (AMED), Japan, and from KAKENHI JP17H01586 (to H.U.) and JP26253077 (to H.U.) from Japan Society for the Promotion of Science (JSPS).
[1]Current affiliation: RIKEN Center for Biosystems Dynamics Research, Kobe, Japan.
[2]Current affiliation: Department of Molecular Pharmacology, Kyoto University Graduate School of Pharmaceutical Sciences, Kyoto, Japan.
[3]Current affiliation: Department of Cellular Neuropathology, Brain Research Institute, Niigata University, Niigata, Japan.
https://doi.org/10.1124/jpet.120.265942.
[S] This article has supplemental material available at jpet.aspetjournals.org.

ABBREVIATIONS: a-CSF, artificial cerebrospinal fluid; ADRA2A, adrenergic α2a receptor; FM, fibromyalgia; GAPDH, glyceraldehyde 3-phosphate dehydrogenase; 5-HT, 5-hydroxytriptamine; ICS, intermittent cold stress; IPS, intermittent psychological stress; LHb, lateral habenula; LPA_1, lysophosphatidic acid receptor 1; MOPr, μ opioid receptor; PAG, periaqueductal gray; PCR, polymerase chain reaction; PVA, paraventricular thalamic nucleus, anterior part; siRNA, small interfering RNA; SNRI, serotonin and norephinephrine reuptake inhibitor.

morphine (Furuta et al., 2009). An acid-saline–induced pain model (Sluka et al., 2001), which shows chronic widespread pain, is sensitive to antidepressants, gabapentinoids (Yokoyama et al., 2007; Kim et al., 2009; DeSantana et al., 2013), and morphine (Sluka et al., 2002). In addition to these, a reserpine-induced biogenic amine depletion model and intermittent sound stress model have been reported, and some pathophysiological and pharmacotherapeutic studies have been discussed (Khasar et al., 2009; Nagakura et al., 2009). We have also added two different FM-like pain models using intermittent cold stress (ICS) and intermittent psychologic stress (IPS) models (Nishiyori and Ueda, 2008; Ueda and Neyama, 2017). The advantages of our model (ICS and IPS) are observed in the pathophysiologic and pharmacotherapeutic features, which include female predominance as well as generalized and chronic pain, and lack of morphine analgesia, despite potent antinociceptive actions of gabapentinoids and reuptake inhibitor–type antidepressants, in agreement with clinical observations (Clauw, 2014; Schrepf et al., 2016). We also found that the mechanisms underlying chronic pain and lack of morphine analgesia are distinct from each other in several studies using ICS model, which demonstrated that repeated administration with pregabalin or donepezil completely reversed the ICS-induced chronic pain lasting several days after the cessation of treatments, whereas the lack of morphine (intracerebroventricular) analgesia still remained (Mukae et al., 2015; Neyama et al., 2020). Such discrepant mechanisms were also observed when the study was performed in lysophosphatidic acid receptor 1 (LPA_1)–deficient mice (Neyama et al., 2020), which have been reported to completely block the hyperalgesia in various neuropathic pain models (Inoue et al., 2004; Uchida et al., 2014; Ueda, 2017; Ueda et al., 2018a,b).

In recent years, several medicines became available to treat the refractory pain in patients with FM. Approved medicines include anticonvulsant pregabalin and antidepressant milnacipran or duloxetine, which have serotonin and norepinephrine reuptake inhibitor activity. Treatment with these medicines has impacted patients with FM (Clauw, 2014; Welsch et al., 2018), although the satisfying improvement of quality of life has not been yet reached due to their side effects (Welsch et al., 2018). The present study is designed to see whether experimental fibromyalgia-like abnormal pain behaviors in the ICS model could be suppressed by an antidepressant mirtazapine, whose pharmacological mechanisms underlying antidepression activity are explained by the disinhibition of 5-hydroxytriptamine (5-HT) release by blocking presynaptic $\alpha 2$ receptor and blockade of postsynaptic excitatory 5-HT2 and 5-HT3 receptors, so that the 5-HT1 receptor–mediated inhibitory signal becomes predominant (Nutt, 1997; Anttila and Leinonen, 2001). In addition, we also discuss the discrepancy of mechanisms underlying chronic pain and lack of morphine analgesia through the pharmacological study using mirtazapine.

Materials and Methods

Animals. Male C57BL/6J mice weighing 20–25 g (6–10 week) were purchased from TEXAM (Nagasaki, Japan). They were kept in a room with a temperature of 21 ± 2°C with free access to a standard laboratory diet and sterile tap water. All experiments were carried out blind.

All experiments were performed after approved by the Nagasaki University Animal Care Committee (number: 1607201325-8) and complied with the recommendations of the International Association for the Study of Pain (Zimmermann, 1983). All study using animals is reported in accordance with the Animal Research: Reporting In Vivo Experiments guideline (Kilkenny et al., 2010; McGrath et al., 2010; McGrath and Lilley, 2015).

Drug Treatments. Drugs were administrated through i.p. (100 μl/10 g body weight) and i.c.v. and i.t. (5 μl) routes. Mirtazapine, kindly provided by Meiji Seika Pharma Co., Ltd. (Kanagawa, Japan), was dissolved in saline containing 0.5% methylcellulose for intraperitoneal injection and in the artificial cerebrospinal fluid (a-CSF; 125 mM NaCl, 3.8 mM, KCl, 1.2 mM KH_2PO_4, 26 mM $NaHCO_3$, 10 mM glucose, pH 7.4) containing 0.5% DMSO (Nacalai Tesque, Kyoto, Japan) for i.c.v. injection.

Intermittent Cold Stress Exposure. Mice were exposed to ICS as previously reported (Nishiyori and Ueda, 2008; Neyama et al., 2020). Briefly, mice were placed in a cold room at 4°C overnight (from 4:30 PM to 10:00 AM), followed by alternating environmental temperatures between 24 and 4°C every 30 minutes from 10:00 AM to 4:30 PM. This was repeated twice on consecutive days. On day 3, the mice were returned to their home cage and adapted to a room, at 24°C, for 1 hour, before the behavioral studies. We designated the third day after the onset of stress exposure as post–stress exposure day (P) 1. Mice in the control group were kept at 24°C for all 3 days (from 4:30 PM on day 1 to 10:00 AM on day 3). During the stress period, two mice were kept in each cage (12 × 15 × 10.5 cm) with free access to food and agar in place of water.

Intermittent Psychologic Stress Exposure. Mice were exposed to intermittent psychologic stress by using the communication box (CBX-9M; Muromachi-Kikai, Tokyo, Japan) that has nine compartments (10 × 10 cm) divided by transparent plastic walls, as reported previously (Ueda and Neyama, 2017). Electric shocks (0.6 mA), for 1 second, were randomly produced 120 times during 1 hour through the grid floor by a shock generator (CSG-001; Muromachi-Kikai) with cycler timer (CBX-CT; Muromachi-Kikai). Floors of compartments located at the center and the four corners were uncovered for the foot-shock group, whereas the remaining four compartments were covered with plastic plates for the psychologic stress (empathy) group.

Small Interfering RNA. The in vivo small interfering RNA (siRNA) delivery using JetSI (Polyplus Transfection, France) was performed as previously reported (Neyama et al., 2020). To confirm the brain locus of microinjected siRNA (0.1 μg/μl), 0.2% of Evans blue was added to the final solution. We used siRNA for adrenergic $\alpha 2a$ receptor (ADRA2A) (NM_007417, SASI_Mm01_00027654) and control siRNA (SIC001), which were purchased from Sigma Genosys (Sigma Aldrich).

Nociception Tests. The threshold of thermal nociception test (Hargreaves test) was evaluated by the latency of paw withdrawal upon thermal stimulus (Hargreaves et al., 1988; Neyama et al., 2020). Mouse were placed in plexiglass cages on top of a glass sheet and habituated 1–3 hours there. The thermal stimulator (IITC Inc., Woodland Hills, CA) was positioned under the glass sheet, and the focus of the projection bulb was aimed exactly at the middle of the plantar surface of the animal. A mirror attached to the stimulator permitted visualization of the plantar surface. In this apparatus, the regulator was set at intensity 20, which increases the plantar surface temperature to 45.1 ± 1.3°C (n = 10) at 10 seconds after the start of thermal stimulation (Neyama et al., 2020). A cutoff time of 20 seconds was set to prevent tissue damage.

In the mechanical nociception test, the stimulus using an electronic von Frey anesthesiometer with rigid tips (Model 2390, 90 g probe 0.8 mm in outer diameter; IITC Inc.) was delivered to the middle of the plantar surface of the right hind paw (Ueda and Neyama, 2017). The pressure needed to induce a withdrawal response was defined as the mechanical pain threshold.

Quantitative Real-Time Polymerase Chain Reaction. Total RNA was prepared from mouse brain tissues, including habenula, mediodorsal thalamus, hippocampus, ventral posterolateral nucleus of thalamus, amygdala, medial hypothalamus, and lateral hypothalamus (from bregma −1.46 to −1.82 mm); insula cortex (from bregma

1.7 to 1.94 mm); paraventricular thalamic nucleus, anterior part (PVA), paraventricular nucleus, and somatosensory cortex S1/S2 (from bregma −0.46 to −0.82 mm); anterior cingulate cortex (from bregma 0.62 to 0.86 mm); periaqueductal gray (PAG; from bregma −3.28 to −3.52 mm); parabrachial nucleus (from bregma −4.96 to ∼5.20 mm); and locus coeruleus and rostroventromedial medulla (from bregma −5.4 to −5.68 mm) (Paxinos and Franklin, 2001) by use of RNeasy Mini Kit (QIAGEN, Tokyo, Japan). To avoid genomic DNA contamination, samples were treated with RNase-Free DNase Kit (QIAGEN). Reverse transcription was carried out by using PrimeScript RT Reagent Kit (Takara Bio Inc., Kusatsu, Japan), and the polymerase chain reaction (PCR) amplification of cDNA was performed with Eco Real-Time PCR System (Illumina, San Diego, CA) and GeneAce SYBR qPCR Mix II (Nippon Gene, Tokyo, Japan). Glyceraldehyde 3-phosphate dehydrogenase (GAPDH) was used as an internal control for normalization. Primer sequences used in this study were as follows: GAPDH, 5′-TATGACTCCACTCACGGCAAAT-3′ (forward), 5′-GGGTCTCGCTCCTGGAAGAT-3′ (reverse); ADRA2A, 5′-TAGAACTGACTTTTCTTCCGTTCTC-3′ (forward), 5′-AACATACA CGCTCTTCTTCAAGC-3′ (reverse); ADRA2B, 5′-CCATCACCTTTC TCATCCT-3′ (forward), 5′-AACACAGCCAGAATTACCA-3′ (reverse); ADRA2C, 5′-ATCTACACTTGTCTTCAATCAGG-3′ (forward), 5′-TCC TTCGAAAGCGGATACGC-3′ (reverse); serotonin 5-HT2a receptor, 5′-CTGCTGGGTTTCCTTGTCAT-3′ (forward), 5′-GTAAATCCA GACGGCACAGAG-3′ (reverse); serotonin 5-HT3a receptor, 5′-CAATGAGTTTGTGGACGTG-3′ (forward), 5′-TTGTAGTTCTGA ACTTCACCTC-3′ (reverse); μ opioid receptor (MOPr), 5′-TTCACC CTCTGCACCATGAGT-3′ (forward), 5′-AGAGAACGTGAGGGT GCAATCT-3′ (reverse); H1, 5′-CAGACCTGATTGTAGGGGCAG-3′ (forward), 5′-CATAGAGAGCCAAAAGAGGCAG-3′ (reverse). In all primer pairs, the presence of a single peak in the melting temperature analysis and linear amplification with increasing number of PCR cycles were validated.

Stereotaxic In Vivo Microinjection. Stereotaxic microinjection into the habenula at P3 after the ICS was performed as previously described (Neyama et al., 2020). The RNA free water solution containing siRNA in 500 nl was injected per site bilaterally to the habenula in a speed of 500 nl/min using a glass micropipette made by a PN-30 micropipette puller (NARISHIGE, Tokyo, Japan) under anesthesia with pentobarbital (Nacalai Tesque) 50 mg/kg, i.p. Stereotaxic coordinates targeted to the habenula were −1.58 to −2.06 mm anterior from the bregma, ± 0.5 to ± 0.3 mm lateral from the midline, and 2.5–2.75 mm ventral from the brain surface at the bregma according to a mouse brain atlas (Paxinos and Franklin, 2001). Immediately after the behavioral test (P5, 2 days after the microinjection), the mouse was sacrificed and the isolated brain dissected, followed by the visual assessment of exact loci of delivered siRNA with Evans blue (0.2%).

Statistical Analysis. Data were calculated by Graphpad Prism 8.0 software (Graphpad Software, San Diego, CA) using the unpaired *t* test, one-way ANOVA with Tukey's multiple comparisons test or Dunnett's multiple comparisons test, two-way ANOVA with Tukey's or Bonferroni's or Dunnett's multiple comparisons test. All data are presented as means ± S.E.M. Differences with *P* value of less than 0.05 were considered statistically significant.

Results

Blockade of ICS-Induced Hyperalgesia by Mirtazapine Treatment. As previously reported (Nishiyori and Ueda, 2008; Neyama et al., 2020), the potent thermal

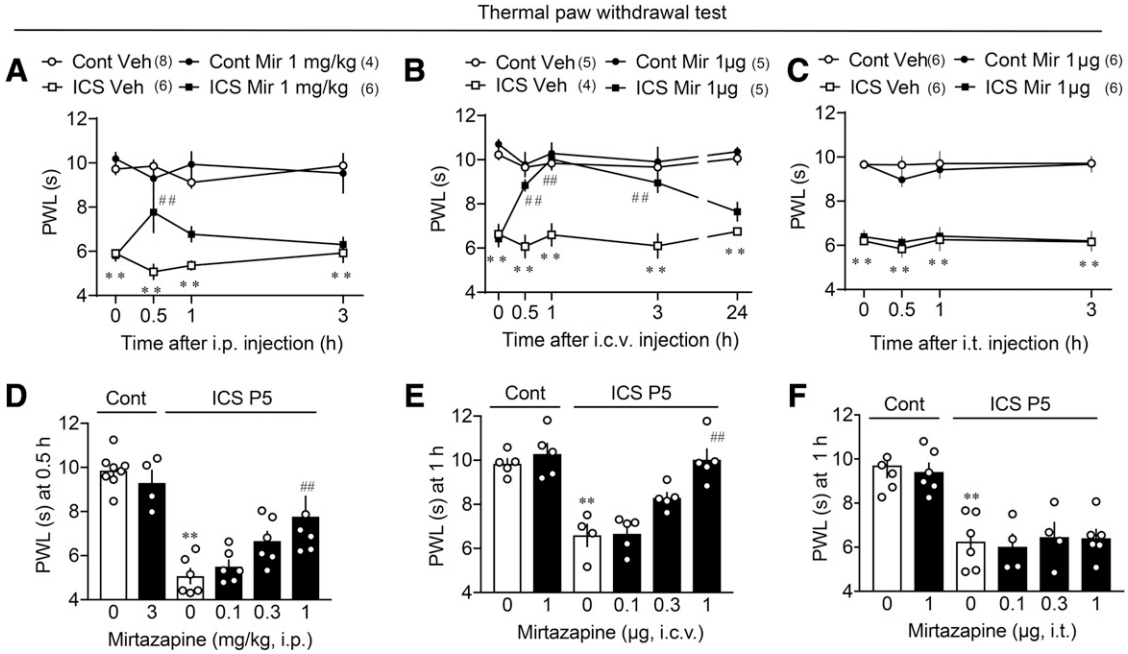

Fig. 1. Blockade of ICS-induced hyperalgesia by brain mirtazapine treatment. (A–C) Time course of nociceptive latency after the administration of mirtazapine (Mir) in the thermal withdrawal test. Results represent the paw withdrawal latency/PWL (s) at indicated time points after vehicle (Veh) or Mir administration at the time point of P5 in control (Cont) and ICS mice. The doses of Mir and administration routes were 1 mg/kg, i.p. (A), 1 μg, i.c.v. (B), and 1 μg, i.t. (C), respectively. The number in parenthesis indicates the number of mice in each group. (D–F) Dose-dependent antihyperalgesic effects of Mir through different administration routes at P5 in ICS mice. Results represent the thermal threshold at 0.5, 1, and 0.5 hour after Mir intraperitoneal, intracerebroventricular, and intrathecal administration, respectively. (A–C) $^{**}P < 0.01$; $^{*}P < 0.05$, vs. Cont Veh, $^{\#\#}P < 0.01$; $^{\#}P < 0.05$, vs. ICS Veh, two-way ANOVA followed by Tukey's multiple comparisons test [(A): interaction $F_{9,\ 79} = 2.079$, $P = 0.0412$; time: $F_{3,\ 79} = 0.1549$, $P = 0.9262$, treatment: $F_{3,\ 79} = 102.6$, $P < 0.0001$; (B): interaction $F_{12,\ 75} = 4.130$, $P < 0.0001$, time $F_{4,\ 75} = 1.797$, $P = 0.1383$, treatment $F_{3,\ 75} = 85.53$, $P < 0.0001$; (C): $F_{9,\ 80} = 0.1764$, $P = 0.9960$, time $F_{3,\ 80} = 0.7303$, $P = 0.5369$, treatment $F_{3,\ 80} = 116$, $P < 0.0001$). (D–F) $^{**}P < 0.01$; $^{*}P < 0.05$, vs. Mir dose 0 (Vehicle) at Cont $^{\#\#}P < 0.01$; $^{\#}P < 0.05$, vs. Mir dose 0 (Vehicle) at ICS P5, one-way ANOVA followed by Tukey's multiple comparisons test [(D): $F_{5,\ 30} = 15.86$, $P < 0.0001$; (E): $F_{5,\ 23} = 18.34$, $P < 0.0001$; (F): $F_{5,\ 26} = 11.85$, $P < 0.0001$].

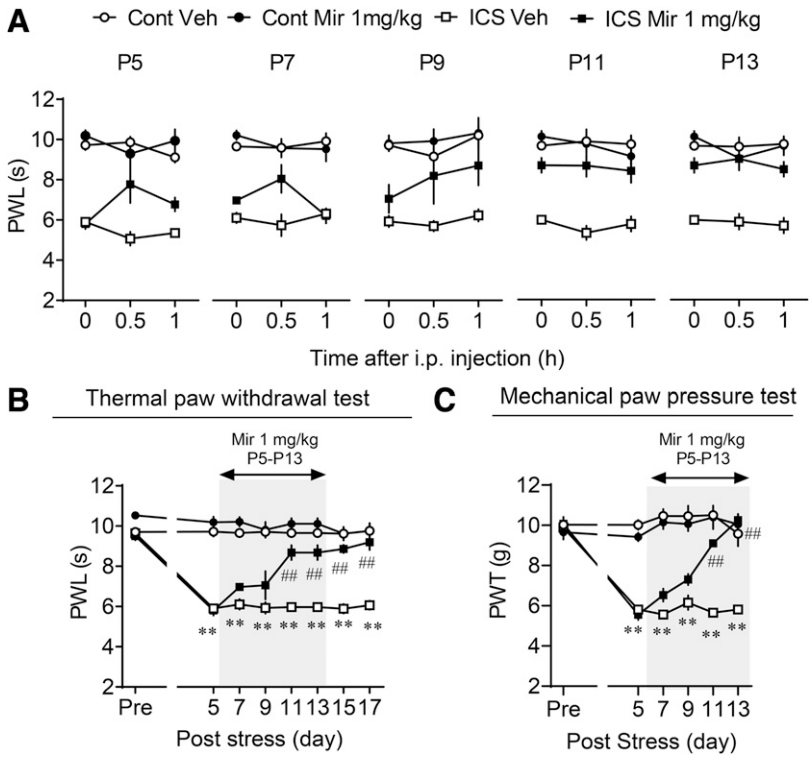

Fig. 2. Long-lasting reversal of hyperalgesia after repeated treatments with Mir in the ICS model. (A) Time course of change in nociceptive latency induced by Mir (1 mg/kg, i.p.) given at P5, 7, 9 11, and 13 in the thermal withdrawal test. (B and C) Chronological change of basal thermal (B) or mechanical (C) nociceptive threshold at time points prior to each Mir administration (P5, 7, 9, and 11) and at P13, 15, and 17. (B and C) $^{**}P < 0.01$, vs. Cont Veh, $^{\#\#}P < 0.01$, vs. ICS Veh, two-way ANOVA followed by Tukey's multiple comparisons test [(B): Interaction $F_{21,\ 154} = 10.33$, $P < 0.0001$, time $F_{7,\ 154} = 18.69$, $P < 0.0001$, treatment $F_{3,\ 154} = 307.6$, $P < 0.0001$; (C): Interaction $F_{15,\ 72} = 13.88$, $P < 0.0001$, time $F_{5,\ 72} = 20.76$, $P < 0.0001$, treatment $F_{3,\ 72} = 162.2$, $P < 0.0001$]. Cont, control; Mir, mirtazapine; Veh, vehicle.

hyperalgesia was observed at the time point of day 5 (P5) after the ICS in mice (Fig. 1A). When mirtazapine at 1 mg/kg was given i.p., significant reversal of hyperalgesia with peak effect at 0.5 hour was observed, compared with the threshold at ICS vehicle treatment. The antihyperalgesic effect gradually declined and reverted to the vehicle control level at 3 hours (Fig. 1A). Mirtazapine has no significant action in control mice. The i.c.v. injection of mirtazapine at 1 μg showed longer antihyperalgesic effect, as shown in Figure 1B. The peak effect was observed at 1 hour, still significant at 3 hours. On the other hand, there was no significant antihyperalgesic effect with the intrathecal treatment (Fig. 1C). A dose-related antihyperalgesic action of mirtazapine was observed for 0.1–1 mg/kg, i.p. (Fig. 1D) and 0.1–1 μg i.c.v. (Fig. 1E), but not at doses up to 1 μg i.t. (Fig. 1F). Similar results were also observed in the mechanical paw pressure test (Supplemental Fig. 1).

Long-Lasting Reversal of Hyperalgesia by Repeated Mirtazapine Treatment. When mirtazapine (1 mg/kg, i.p.) was given every other day from P5 to P13, the thermal nociceptive threshold before each treatment (basal threshold) gradually increased in ICS model, but not in control mice, as shown in Figure 2A. No mirtazapine-induced acute change in threshold was observed on P11 or P13. The plot of chronological change in the basal threshold showed the complete recovery of thermal and mechanical nociceptive threshold by the time of P13 and for 4 more days after the cessation of mirtazapine treatments (Fig. 2, B and C).

Recovery of Morphine Analgesia after Repeated Treatment with Mirtazapine. As previously reported (Nishiyori et al., 2010; Neyama et al., 2020), brain morphine analgesia (0.3 nmol, i.c.v.) in the thermal nociception test was completely lost in ICS mice (Fig. 3, A and C). When mirtazapine (1 mg/kg, i.p.) was repeatedly administered from P5 to P13, there was a complete recovery of morphine analgesia. As well as the complete reversal of hyperalgesia at P18, in ICS mice, no change in the basal nociceptive threshold or morphine analgesia was observed in control mice treated with repeated mirtazapine (Fig. 3, D and E), compared with the cases treated with vehicle (Fig. 3, B and D). Figure 3F shows the quantitative analyses of repeated mirtazapine-induced reversal of hyperalgesia and recovery of morphine analgesia. Quite similar results were also observed when IPS-induced hyperalgesia was evaluated, where the mirtazapine treatments completely reversed the thermal hyperalgesia and recovered morphine analgesia (Fig. 3G).

Upregulation of Adrenergic α2a Receptor Gene Expression in the Habenula after ICS Exposure. The above findings prompted us to test whether ICS exposure could affect the expression levels of mirtazapine target receptors, which include central adrenergic α2, serotonergic 5HT2, 5-HT3, and histaminergic H1 receptors (Nutt, 1997). To this end, we performed quantitative PCR to measure their mRNA levels in 16 pain-related brain regions from control and ICS-treated mice. As shown in Figure 4, among the brain regions the habenula was the only region showing time-dependent upregulation of α2a receptor mRNA, which started at P1 and lasted through P12 after ICS exposure. On the other hand, we found no substantial increase of α2b or α2c receptor gene expression throughout 16 brain regions and time points, except for a very weak increase of gene expression of α2b in habenula at P5 and PVA at P12 and α2c in PVA at P1 (Supplemental Figs. 3 and 4). Regarding 5-HT2a and 5-HT3a gene expression, there was transient upregulation only at the early stage day 2 (D2) and/or P1, as shown in Supplemental Figs. 5 and 6. There was no significant change in H1 receptor gene expression throughout all preparations

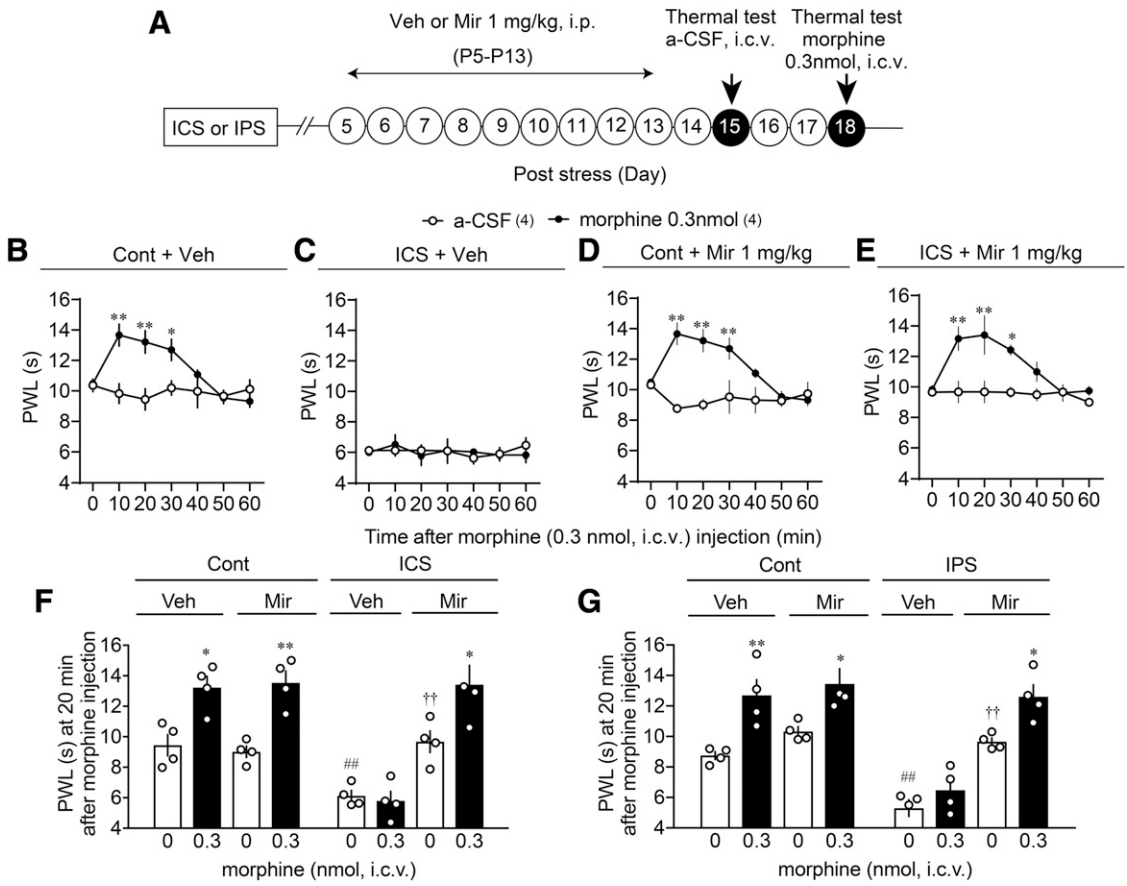

Fig. 3. Recovery of morphine analgesia after repeated treatments with Mir. (A) Time schedule of Mir treatment, nociceptive, and morphine analgesia test in ICS or IPS mice. (B–E) Time course of nociceptive threshold after the intracerebroventricular administration of a-CSF (P15) or morphine (P18) in the thermal withdrawal test in Cont (B) or ICS (C) mice treated (P5–12) with Veh (B and C) or Mir (D and E). (F) Quantitative comparison of morphine analgesia in Cont or ICS mice pretreated with Veh or Mir. (G) Quantitative comparison of morphine analgesia in Cont or IPS mice pretreated with Veh or Mir. (B, D, and E) $^{**}P < 0.01$; $^{*}P < 0.05$, vs. a-CSF, two-way ANOVA followed by Bonferroni's multiple comparisons test [(B): Interaction $F_{6, 42} = 5.056$, $P = 0.0006$, time $F_{6, 42} = 4.033$, $P = 0.0028$, treatment $F_{1, 42} = 21.59$, $P < 0.0001$; (D): Interaction $F_{6, 42} = 6.498$, $P < 0.0001$, time $F_{6, 42} = 3.353$, $P = 0.0086$, treatment $F_{1, 42} = 40.63$, $P < 0.0001$; (E): Interaction $F_{6, 42} = 3.640$, $P = 0.0053$, time $F_{6, 42} = 4.767$, $P = 0.0009$, treatment $F_{1, 42} = 32.27$, $P < 0.0001$]. (F and G) $^{**}P < 0.01$; $^{*}P < 0.05$, vs. morphine dose 0 (a-CSF) at each corresponding column, $^{\#\#}P < 0.01$, vs. morphine dose 0, Cont, Veh, $^{\dagger\dagger}P < 0.01$, vs. morphine dose 0, ICS/IPS, Veh, unpaired t test. Cont, control; Mir, mirtazapine; Veh, vehicle.

(Supplemental Fig. 7). Similarly, there was no change in MOPr gene expression except for the case of D2 in amygdala (Supplemental Fig. 8).

Reversal of Hyperalgesia by Microinjection of siRNA ADRA2A. When siRNA for ADRA2A was bilaterally microinjected (0.5 μl each) into habenula at P3 after the ICS (Fig. 5, A and C), significant reversal of hyperalgesia was observed at P5, whereas no significant reversal of hyperalgesia was observed by the microinjection into mediodorsal thalamus (Fig. 5D). However, no significant analgesic action by intracerebroventricular morphine at P5 was observed by the siRNA ADRA2A microinjection into habenula (Fig. 5, E and F).

Reversal of Hyperalgesia and Loss of Morphine Analgesia by Repeated Intracerebroventricular Treatments with siRNA ADRA2A. As shown in Figure 6A, siRNA ADRA2A was administered (intracerebroventricularly) three times, at P3, 5, and 7, to evaluate for the involvement of ADRA2A in the other brain regions in the hyperalgesia and loss of intracerebroventricular morphine analgesia. When siRNA ADRA2A was administered every other day (P3, P5, and P7), the reversal of hyperalgesia was observed at P5, P7, and P9, respectively (Fig. 6B), and the significant recovery of morphine analgesia was observed at P7 and P9.

Discussion

In the present study, using the ICS model of FM we found that the systemic administration of mirtazapine has a potent pharmacotherapeutic action, contrasting with our previous study in which several selective serotonin reuptake inhibitors or serotonin norephinephrine reuptake inhibitors (SNRIs) suppressed the ICS-induced pain after intrathecal, but not systemic administration (Nishiyori and Ueda, 2008). In addition, as mirtazapine-induced beneficial effects were observed when given through an intracerebroventricular route, but not an intrathecal route, the mode or site of action of mirtazapine seems to be different from that for selective serotonin reuptake inhibitors or SNRIs. In our previous study using the IPS model, duloxetine, a frequently used SNRI for patients with FM, showed potent antihyperalgesia by the intrathecal but not intracerebroventricular route of administration (Ueda and Neyama, 2017). The usefulness of

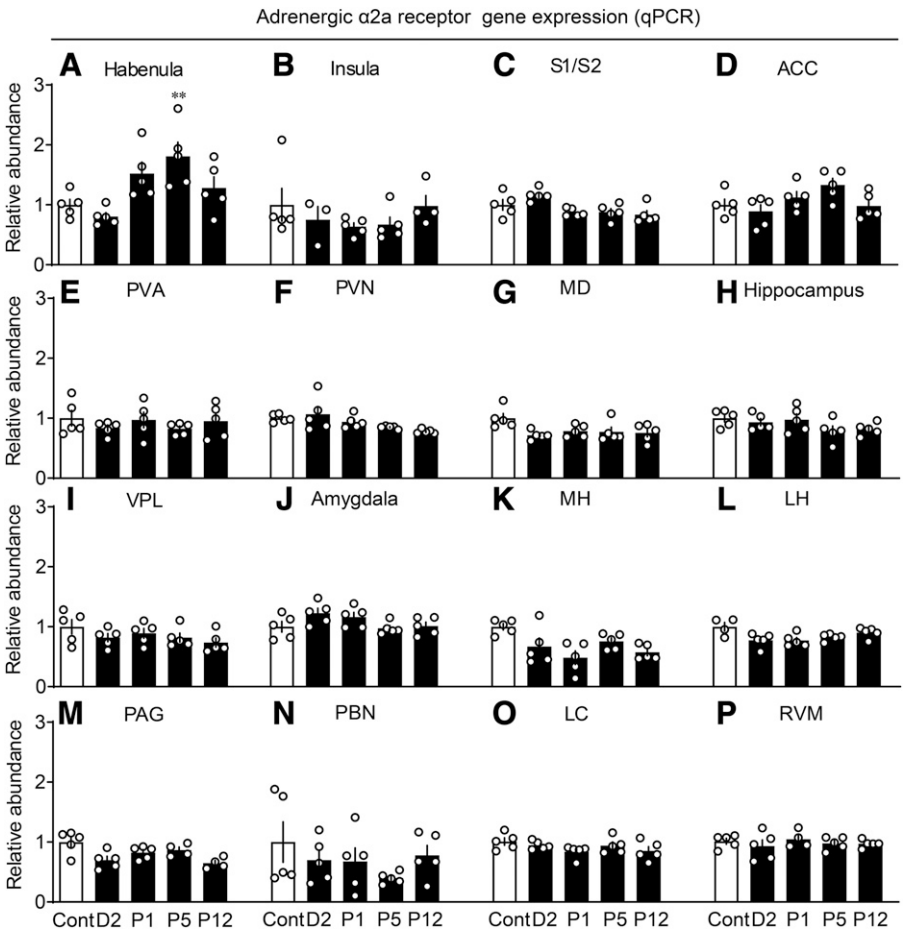

Fig. 4. Upregulation of adrenergic α2a receptor gene expression in the habenula of ICS-treated mice (A–P). Time-course of adrenergic α2a receptor mRNA expression in the brain regions, including habenula (A), insula (B), S1 and S2 cortices (S1/S2) (C), anterior cingulate cortex (ACC) (D), PVA (E), paraventricular nucleus (PVN) (F), mediodorsal thalamus (MD) (G), hippocampus (H), ventral posterolateral nucleus of thalamus (VPL) (I), amygdala (J), medial hypothalamus (MH) (K), lateral hypothalamus (LH) (L), PAG (M), parabrachial nucleus (PBN) (N), locus coeruleus (LC) (O), and RVM (rostroventromedial medulla) (P) after ICS exposure. The mRNA level of adrenergic α2a receptor was quantified by using quantitative PCR (qPCR) and normalized to that of housekeeping gene GAPDH. Data are presented as percentage of each control day and expressed as means ± S.E.M. from at least three mice. (A) $^{**}P < 0.01$, vs. control (Cont), one-way ANOVA followed by Dunnett's multiple comparisons test ($F_{4,\ 42} = 5.832$, $P = 0.0028$).

mirtazapine in clinical practice has been reported in patients with FM (Miki et al., 2016; Ottman et al., 2018; Welsch et al., 2018).

The first observation in the present study demonstrates that adrenergic α2a receptor expression is upregulated in the habenula, in the ICS model. The upregulation was observed at the pain maintenance stage, P5 to P12, as well as P1, in contrast to the data with other mirtazapine target receptors (α2b, α2c, 5-HT2a, 5-HT3a, or H1), which showed no substantial or just transient upregulation. Based on these findings, we knocked down the ADRA2A receptor by use of siRNA microinjection bilaterally into the habenula and successfully obtained the reversal of the hyperalgesia. Regarding the pain-related role of habenula, there are reports that increased pain sensitivity after chronic, unpredictable mild stress (a model of depression) was abolished by the electrolytic lesion of lateral habenula (LHb) (Li et al., 2016) and that various types of chronic pain cause an activation of habenula neurons (Elman et al., 2013; Boulos et al., 2017). These findings suggest that habenula plays roles in the central or emotional pain and analgesia mechanisms during chronic pain (Hikosaka, 2010). Furthermore, it is also reported that both LHb and medial habenula projections contribute to the direct and indirect activation of descending serotonergic pain-inhibitory system through raphe nuclei (dorsal raphe and raphe magnus) and PAG, respectively (Shelton et al., 2012; Metzger et al., 2017), suggesting that the intense or repeated stimulation of habenula disinhibits the descending pain inhibitory system. Regarding possible roles of ADRA2A receptor in habenula, limited information is available, but it is described that high levels of *Adra2a* mRNA are detected in the medial habenula and medial division of LHb of C57BL/6J mouse by in situ hybridization study in the Allen Brain Atlas (https://mouse.brain-map.org/). In addition, there is an interesting report that peripheral damage (superior cervical ganglionectomy) results in increases of norepinephrine levels in habenula (Gottesfeld, 1983), a finding to support the view that noradrenergic system in the habenula is involved in the stress-related pain status (Shelton et al., 2012). In addition to the descending pain inhibitory mechanism, it is interesting to discuss the possibility that mirtazapine may disinhibit the reward-related hypoalgesia through a blockade of habenula–ventral tegmental area transmission (Taylor et al., 2019), since the habenula projects glutamatergic neurons to the ventral tegmental area (Brinschwitz et al., 2010), where GABAergic interneurons inhibit DA release. We should also consider the possible actions of mirtazapine on nonneuronal cells expressing ADRA2A (Mori et al., 2002; Morioka et al., 2014; Caraci et al., 2019) and some contribution of other mirtazapine target receptors (5-HT2a, 5-HT3a), showing transient and sporadic upregulation.

The second observation demonstrates that repeated systemic treatments with mirtazapine for 9 days completely reversed the hyperalgesia, an effect that lasted for at least 4 days even after the cessation of mirtazapine treatments (Fig. 3, B and C). This type of pain memory inhibition was also

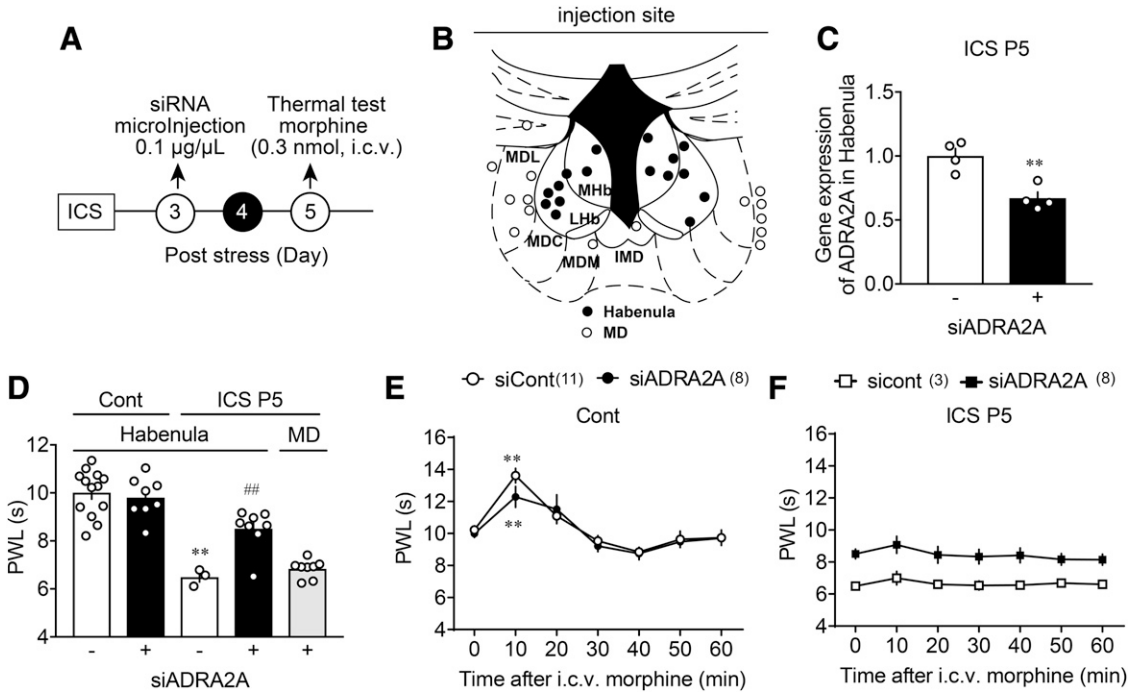

Fig. 5. Reversal of hyperalgesia by microinjection of siRNA ADRA2A. (A) Time schedule of microinjection, nociceptive, and morphine analgesia test. (B) Confirmed sites of siRNA microinjection in habenula area. (C) Decreased ADRA2A gene expression at 2 days (P5) after siRNA microinjection into the habenula of ICS mice. (D) Reversal of thermal hyperalgesia by siRNA ADRA2A into the habenula, but not mediodorsal (MD) thalamus. (E and F) Morphine analgesia in control (Cont) (E) or ICS (F) mice after the microinjection into the habenula. (C) $^{**}P < 0.01$, vs. siADRA2A, unpaired t test. (D) $^{**}P < 0.01$, vs. Cont siADRA2A (-) in habenula, $^{\#\#}P < 0.01$, vs. ICS P5 siADRA2A (-) in habenula, one-way ANOVA followed by Tukey's multiple comparisons test ($F_{4,\ 35} = 28.81$, $P < 0.0001$). (E) $^{**}P < 0.01$, vs. time 0, two-way ANOVA followed by Dunnett's multiple comparisons test (interaction $F_{6,\ 119} = 0.6948$, $P = 0.6543$, time $F_{6,\ 119} = 19.73$, $P < 0.0001$, treatment $F_{1,\ 119} = 1.065$, $P = 3.042$). IMD, intermediodorsal nucleus; MDC, mediodorsal central; MDL, mediodorsal lateral; MDM, mediodorsal medial; siADR2A, siRNA for ADR2A; siCont, siRNA for control.

observed in the IPS model (Supplemental Fig. 2), a model that mimics the pathophysiology (generalized, chronic, and female-predominant pain) and pharmacotherapy (lack of antihyperalgesia by nonsteroidal anti-inflammatory drug diclofenac or morphine) of patients with FM, as previously reported (Ueda and Neyama, 2017). Similar pain memory inhibition after repeated treatments with drugs was observed with pregabalin and donepezil (Mukae et al., 2015, 2016). The complete reversal of ICS-induced hyperalgesia by repeated pregabalin treatments (intracerebroventricularly) was observed at 7 days

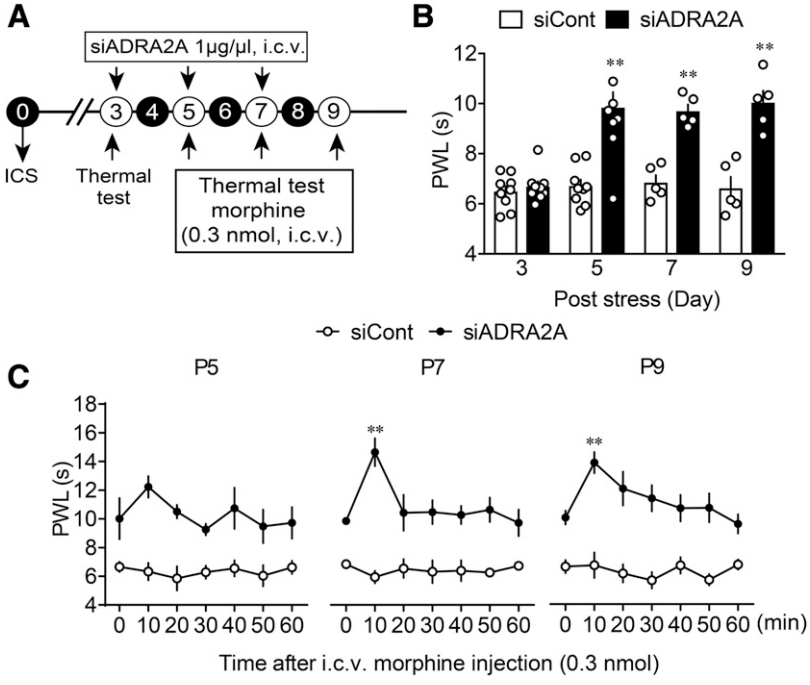

Fig. 6. Reversal of hyperalgesia and loss of morphine analgesia by repeated intracerebroventricular treatments with siRNA ADRA2A. (A) Time schedule of siRNA ADRA2A injection, nociceptive, and morphine analgesia test. (B) Reversal of thermal hyperalgesia by siRNA ADRA2A injection (intracerebroventricularly) in ICS mice. Nociceptive tests at P3, 5, and 7 were performed prior to siRNA injection. (C) Recovery of morphine analgesia at P7 and 9 by repeated siRNA ADRA2A injections (intracerebroventricularly). (B) $^{**}P < 0.01$, vs. siCont at each day, two-way ANOVA followed by Bonferroni's multiple comparisons test (interaction $F_{3,\ 32} = 3.539$, $P = 0.0255$, time: $F_{3,\ 32} = 5.164$, $P = 0.0050$, treatment $F_{1,\ 32} = 45.41$, $P < 0.0001$). (C) $^{**}P < 0.01$, vs. time 0 at each post day, two-way ANOVA followed by Dunnett's multiple comparisons test (P5: interaction $F_{6,\ 49} = 0.8573$, $P = 0.5328$, time: $F_{6,\ 49} = 0.8649$, $P = 0.5273$, treatment $F_{1,\ 49} = 83.82$, $P < 0.0001$, siCont $n = 5$, siADRA2A $n = 4$; P7: interaction $F_{6,\ 49} = 4.020$, $P = 0.0024$, time: $F_{6,\ 49} = 2.258$, $P = 0.0529$, treatment $F_{1,\ 49} = 144.1$, $P < 0.0001$, siCont $n = 5$, siADRA2A $n = 4$; P9: interaction $F_{6,\ 56} = 2.141$, $P = 0.0627$, time: $F_{6,\ 56} = 2.048$, $P = 0.0743$, treatment $F_{1,\ 56} = 151.6$, $P < 0.0001$, $n = 5$).

after the cessation of treatments (Mukae et al., 2016). We have observed the inhibition of ICS hyperalgesia by muscarinic agonist pilocarpine, which is expected to inhibit dry eyes and dry mouth, a symptom observed in patients with fibromyalgia (Mukae et al., 2015). We further observed potent antihyperalgesia with a systemic administration of low dose (10 μg/kg i.p.) of donepezil, which has a good central penetration. The complete reversal of hyperalgesia was also observed at 7 days after the cessation of repeated donepezil treatments (Mukae et al., 2015). Thus, it seems that ICS-induced hyperalgesia and its drug reversibility are attributed to multiple mechanisms in the brain.

The third observation demonstrates that the pharmacotherapeutic feature of mirtazapine is different from other treatments in terms of reestablishing morphine sensitivity. In our previous studies (Mukae et al., 2015; Neyama et al., 2020), there was no significant analgesia by morphine given after the repeated treatments with pregabalin or donepesil, which completely reversed the ICS-induced decrease in basal (or pretreatment) threshold to the naïve level. Through these studies, we have speculated that the complete interruption of feed-forward pain loop by repeated treatments with pain inhibitors reverses the pain threshold to the naïve level (or pain memory) even after the treatments. This view reminds us of the fact that repeated treatments with the antagonist of LPA_1, which is responsible for the development and maintenance of nerve injury–induced neuropathic pain, also reverse the pain threshold to the naive level (Inoue et al., 2004; Ueda et al., 2018a). Recently we have reported that LPA_1 is involved in the development and maintenance in several fibromyalgia-like pain models, including IPS and ICS models (Ueda and Neyama, 2017). Indeed, similar findings were also observed with the study using LPA_1-deficient mice, which abolish the hyperalgesia but still lack morphine analgesia in the ICS model (Neyama et al., 2020). However, in the present study using repeated mirtazapine, there was a complete recovery of central morphine analgesia 6 days after the cessation of repeated mirtazapine, which completely reversed ICS-induced hyperalgesia.

An additional interesting finding in the present study is that the knockdown of adrenergic $\alpha 2$ receptor in the habenula reversed the hyperalgesia but did not recover the loss of morphine analgesia. As there are reports that opioid μ-receptors in multiple brain loci are involved in the morphine analgesia (Basbaum et al., 1976; Takagi et al., 1977; Fardin et al., 1984; Cohen and Melzack, 1985; Jones and Gebhart, 1988; Taylor et al., 2019), we treated with siRNA for the ADRA2A gene, through the intracerebroventricular route, which may cover the knockdown of MOPr at various loci, and successfully obtained the recovery of morphine analgesia in mice, which had been treated with the siRNA. However, the identification of brain loci for the action of siRNA, responsible for recovery of morphine analgesia, remains to be elucidated. Most recently, we have reported that the lack of morphine analgesia is reversed by the microinjection of siRNA for antiopioid *N*-methyl-D-aspartate receptor subtype 2A subunit receptor gene into the PAG (Neyama et al., 2020), but the role of ADRA2A in the PAG in terms of antiopioid systems remains elusive.

Finally, as FM has a female-predominant sex difference (Clauw, 2014), animal studies using female mice are also necessary. We have previously observed that both male and female mice have similar hyperalgesia in ICS and IPS models, but hyperalgesia in male but not female mice is largely attenuated by gonadectomy (Nishiyori and Ueda, 2008; Ueda and Neyama, 2017). Regarding the sexual dimorphism in pain research, there are interesting reports (Sorge et al., 2015; Mapplebeck et al., 2016) that microglia play key roles in the development and maintenance of neuropathic pain in male mice, whereas their roles are negligible in female mice. Instead in female mice, peripheral T cells are reported to play important roles in fibromyalgia in clinic and experimental neuropathic pain model (Rosen et al., 2017; Banfi et al., 2020). Thus, studies composed of another set of experiments for mirtazapine effects using female mice would be the next important subject in combination with the study evaluating the contribution of microglia and T cells.

In conclusion, the present study demonstrated that mirtazapine has beneficial actions in the reversal of hyperalgesia and recovery of morphine analgesia in the ICS- and IPS-induced hyperalgesia. One of mechanisms underlying the reversal of hyperalgesia is the blockade of habenular adrenergic $\alpha 2$ receptor, which is upregulated by ICS exposure. The present findings that the lack of morphine analgesia was reversed by intracerebroventricular administration of siRNA, but not by habenular microinjection, suggest that ICS-induced hyperalgesia and lack of morphine analgesia are attributed to distinct mechanisms through $\alpha 2$ receptor in terms of brain loci.

Acknowledgments

The authors are grateful to Ryoko Tsukahara, Michiko Nishiyori, Jun Nagai, Takehiro Mukae, and Soichiro Kawamoto for the technical helps of real-time PCR and pain behavior tests.

Authorship Contributions

Participated in research design: Neyama, Ueda.
Conducted experiments: Neyama, Dozono, Uchida.
Performed data analysis: Neyama, Dozono, Uchida.
Wrote or contributed to the writing of the manuscript: Uchida, Ueda.

References

Anttila SA and Leinonen EV (2001) A review of the pharmacological and clinical profile of mirtazapine. *CNS Drug Rev* **7**:249–264.
Banfi G, Diani M, Pigatto PD, and Reali E (2020) T cell subpopulations in the physiopathology of fibromyalgia: evidence and perspectives. *Int J Mol Sci* **21**:1186.
Basbaum AI, Bautista DM, Scherrer G, and Julius D (2009) Cellular and molecular mechanisms of pain. *Cell* **139**:267–284.
Basbaum AI, Clanton CH, and Fields HL (1976) Opiate and stimulus-produced analgesia: functional anatomy of a medullospinal pathway. *Proc Natl Acad Sci USA* **73**:4685–4688.
Bennett GJ and Xie YK (1988) A peripheral mononeuropathy in rat that produces disorders of pain sensation like those seen in man. *Pain* **33**:87–107.
Boulos LJ, Darcq E, and Kieffer BL (2017) Translating the habenula-from rodents to humans. *Biol Psychiatry* **81**:296–305.
Brinschwitz K, Dittgen A, Madai VI, Lommel R, Geisler S, and Veh RW (2010) Glutamatergic axons from the lateral habenula mainly terminate on GABAergic neurons of the ventral midbrain. *Neuroscience* **168**:463–476.
Caraci F, Merlo S, Drago F, Caruso G, Parenti C, and Sortino MA (2019) Rescue of noradrenergic system as a novel pharmacological strategy in the treatment of chronic pain: focus on microglia activation. *Front Pharmacol* **10**:1024.
Chen SL, Wu XY, Cao ZJ, Fan J, Wang M, Owyang C, and Li Y (2008) Subdiaphragmatic vagal afferent nerves modulate visceral pain. *Am J Physiol Gastrointest Liver Physiol* **294**:G1441–G1449.
Clauw DJ (2014) Fibromyalgia: a clinical review. *JAMA* **311**:1547–1555.
Cohen SR and Melzack R (1985) Morphine injected into the habenula and dorsal posteromedial thalamus produces analgesia in the formalin test. *Brain Res* **359**:131–139.
Costigan M, Scholz J, and Woolf CJ (2009) Neuropathic pain: a maladaptive response of the nervous system to damage. *Annu Rev Neurosci* **32**:1–32.
DeSantana JM, da Cruz KM, and Sluka KA (2013) Animal models of fibromyalgia. *Arthritis Res Ther* **15**:222.

Devor M (2013) Neuropathic pain: pathophysiological response of nerves to injury, in *Wall and Melzack's Textbook of Pain*, 6th ed (McMahon SB, Tracey KMI, and Turk DC eds), pp 861–888, Elsevier, Philadelphia, PA.
Elman I, Borsook D, and Volkow ND (2013) Pain and suicidality: insights from reward and addiction neuroscience. *Prog Neurobiol* **109**:1–27.
Fardin V, Oliveras JL, and Besson JM (1984) A reinvestigation of the analgesic effects induced by stimulation of the periaqueductal gray matter in the rat. II. Differential characteristics of the analgesia induced by ventral and dorsal PAG stimulation. *Brain Res* **306**:125–139.
Furuta S, Shimizu T, Narita M, Matsumoto K, Kuzumaki N, Horie S, Suzuki T, and Narita M (2009) Subdiaphragmatic vagotomy promotes nociceptive sensitivity of deep tissue in rats. *Neuroscience* **164**:1252–1262.
Gottesfeld Z (1983) Central and peripheral contributions of deafferentation-induced norepinephrine increase in the habenula. *Brain Res* **268**:359–361.
Hargreaves K, Dubner R, Brown F, Flores C, and Joris J (1988) A new and sensitive method for measuring thermal nociception in cutaneous hyperalgesia. *Pain* **32**:77–88.
Hikosaka O (2010) The habenula: from stress evasion to value-based decision-making. *Nat Rev Neurosci* **11**:503–513.
Hill RG (2013) Analgesic drugs in development, in *Wall and Melzack's Textbook of Pain*, 6th ed (McMahon SB and Tracey KM I, and Turk DC eds), pp 552–562, Elsevier, Philadelphia, PA.
Inoue M, Rashid MH, Fujita R, Contos JJ, Chun J, and Ueda H (2004) Initiation of neuropathic pain requires lysophosphatidic acid receptor signaling. *Nat Med* **10**:712–718.
Jones SL and Gebhart GF (1988) Inhibition of spinal nociceptive transmission from the midbrain, pons and medulla in the rat: activation of descending inhibition by morphine, glutamate and electrical stimulation. *Brain Res* **460**:281–296.
Khasar SG, Dina OA, Green PG, and Levine JD (2009) Sound stress-induced long-term enhancement of mechanical hyperalgesia in rats is maintained by sympathoadrenal catecholamines. *J Pain* **10**:1073–1077.
Khasar SG, Miao FJ, Jänig W, and Levine JD (1998a) Vagotomy-induced enhancement of mechanical hyperalgesia in the rat is sympathoadrenal-mediated. *J Neurosci* **18**:3043–3049.
Khasar SG, Miao JP, Jänig W, and Levine JD (1998b) Modulation of bradykinin-induced mechanical hyperalgesia in the rat by activity in abdominal vagal afferents. *Eur J Neurosci* **10**:435–444.
Kilkenny C, Browne W, Cuthill IC, Emerson M, and Altman DG; NC3Rs Reporting Guidelines Working Group (2010) Animal research: reporting in vivo experiments: the ARRIVE guidelines. *Br J Pharmacol* **160**:1577–1579.
Kim SH, Song J, Mun H, and Park KU (2009) Effect of the combined use of tramadol and milnacipran on pain threshold in an animal model of fibromyalgia. *Korean J Intern Med (Korean Assoc Intern Med)* **24**:139–142.
Kuner R (2010) Central mechanisms of pathological pain. *Nat Med* **16**:1258–1266.
Li J, Li Y, Zhang B, Shen X, and Zhao H (2016) Why depression and pain often coexist and mutually reinforce: role of the lateral habenula. *Exp Neurol* **284** (Pt A): 106–113.
Mapplebeck JC, Beggs S, and Salter MW (2016) Sex differences in pain: a tale of two immune cells. *Pain* **157** (Suppl 1):S2–S6.
McGrath JC, Drummond GB, McLachlan EM, Kilkenny C, and Wainwright CL (2010) Guidelines for reporting experiments involving animals: the ARRIVE guidelines. *Br J Pharmacol* **160**:1573–1576.
McGrath JC and Lilley E (2015) Implementing guidelines on reporting research using animals (ARRIVE etc.): new requirements for publication in BJP. *Br J Pharmacol* **172**:3189–3193.
Metzger M, Bueno D, and Lima LB (2017) The lateral habenula and the serotonergic system. *Pharmacol Biochem Behav* **162**:22–28.
Miki K, Murakami M, Oka H, Onozawa K, Yoshida S, and Osada K (2016) Efficacy of mirtazapine for the treatment of fibromyalgia without concomitant depression: a randomized, double-blind, placebo-controlled phase IIa study in Japan. *Pain* **157**: 2089–2096.
Mori K, Ozaki E, Zhang B, Yang L, Yokoyama A, Takeda I, Maeda N, Sakanaka M, and Tanaka J (2002) Effects of norepinephrine on rat cultured microglial cells that express alpha1, alpha2, beta1 and beta2 adrenergic receptors. *Neuropharmacology* **43**:1026–1034.
Morioka N, Abe H, Araki R, Matsumoto N, Zhang FF, Nakamura Y, Hisaoka-Nakashima K, and Nakata Y (2014) A β1/2 adrenergic receptor-sensitive intracellular signaling pathway modulates CCL2 production in cultured spinal astrocytes. *J Cell Physiol* **229**:323–332.
Mukae T, Fujita W, and Ueda H (2016) P-glycoprotein inhibitors improve effective dose and time of pregabalin to inhibit intermittent cold stress-induced central pain. *J Pharmacol Sci* **131**:64–67.
Mukae T, Uchida H, and Ueda H (2015) Donepezil reverses intermittent stress-induced generalized chronic pain syndrome in mice. *J Pharmacol Exp Ther* **353**: 471–479.
Nagakura Y, Oe T, Aoki T, and Matsuoka N (2009) Biogenic amine depletion causes chronic muscular pain and tactile allodynia accompanied by depression: a putative animal model of fibromyalgia. *Pain* **146**:26–33.
Neyama H, Dozono N, and Ueda H (2020) NR2A-NMDA receptor blockade reverses the lack of morphine analgesia without affecting chronic pain status in a fibromyalgia-like mouse model. *J Pharmacol Exp Ther* **373**:103–112.
Nishiyori M, Nagai J, Nakazawa T, and Ueda H (2010) Absence of morphine analgesia and its underlying descending serotonergic activation in an experimental mouse model of fibromyalgia. *Neurosci Lett* **472**:184–187.
Nishiyori M and Ueda H (2008) Prolonged gabapentin analgesia in an experimental mouse model of fibromyalgia. *Mol Pain* **4**:52.
Nutt D (1997) Mirtazapine: pharmacology in relation to adverse effects. *Acta Psychiatr Scand Suppl* **391**:31–37.
Ossipov MH and Porreca F (2013) Animal models of experimental neuropathic pain, in *Wall and Melzack's Textbook of Pain*, 6th ed (McMahon SB, Tracey I, and Turk DC eds), pp 889–901, Elsevier, Philadelphia, PA.
Ottman AA, Warner CB, and Brown JN (2018) The role of mirtazapine in patients with fibromyalgia: a systematic review. *Rheumatol Int* **38**:2217–2224.
Paxinos G and Franklin KBJ (2001) *The Mouse Brain in Stereotaxic Coordinates*, Academic Press, San Diego, CA.
Rosen S, Ham B, and Mogil JS (2017) Sex differences in neuroimmunity and pain. *J Neurosci Res* **95**:500–508.
Russell IJ (2005) Neurotransmitters, cytokines, hormones and the immune system in chronic neuropathic pain, in *Fibromyalgia and Other Central Pain Syndromes* (Wallace DJ and Clauw DJ 63–79, Lippincott Williams & Wilkins, Philadelphia, PA.
Russell IJ (2013) Fibromyalgia syndrome and myofascial pain syndrome, in *Wall and Melzack's Textbook of Pain*, 6th ed (McMahon SB, Tracey I, and Turk DC eds), pp 658–682, Elsevier, Philadelphia, PA.
Schrepf A, Harper DE, Harte SE, Wang H, Ichesco E, Hampson JP, Zubieta JK, Clauw DJ, and Harris RE (2016) Endogenous opioidergic dysregulation of pain in fibromyalgia: a PET and fMRI study. *Pain* **157**:2217–2225.
Shelton L, Becerra L, and Borsook D (2012) Unmasking the mysteries of the habenula in pain and analgesia. *Prog Neurobiol* **96**:208–219.
Sluka KA and Clauw DJ (2016) Neurobiology of fibromyalgia and chronic widespread pain. *Neuroscience* **338**:114–129.
Sluka KA, Kalra A, and Moore SA (2001) Unilateral intramuscular injections of acidic saline produce a bilateral, long-lasting hyperalgesia. *Muscle Nerve* **24**:37–46.
Sluka KA, Rohlwing JJ, Bussey RA, Eikenberry SA, and Wilken JM (2002) Chronic muscle pain induced by repeated acid Injection is reversed by spinally administered mu- and delta-, but not kappa-, opioid receptor agonists. *J Pharmacol Exp Ther* **302**:1146–1150.
Sorge RE, Mapplebeck JC, Rosen S, Beggs S, Taves S, Alexander JK, Martin LJ, Austin JS, Sotocinal SG, Chen D, et al. (2015) Different immune cells mediate mechanical pain hypersensitivity in male and female mice. *Nat Neurosci* **18**: 1081–1083.
Takagi H, Satoh M, Akaike A, Shibata T, and Kuraishi Y (1977) The nucleus reticularis gigantocellularis of the medulla oblongata is a highly sensitive site in the production of morphine analgesia in the rat. *Eur J Pharmacol* **45**:91–92.
Taylor NE, Long H, Pei J, Kukutla P, Phero A, Hadaegh F, Abdelnabi A, Solt K, and Brenner GJ (2019) The rostromedial tegmental nucleus: a key modulator of pain and opioid analgesia. *Pain* **160**:2524–2534.
Uchida H, Nagai J, and Ueda H (2014) Lysophosphatidic acid and its receptors LPA1 and LPA3 mediate paclitaxel-induced neuropathic pain in mice. *Mol Pain* **10**:71.
Ueda H (2006) Molecular mechanisms of neuropathic pain-phenotypic switch and initiation mechanisms. *Pharmacol Ther* **109**:57–77.
Ueda H (2008) Peripheral mechanisms of neuropathic pain - involvement of lysophosphatidic acid receptor-mediated demyelination. *Mol Pain* **4**:11.
Ueda H (2017) Lysophosphatidic acid signaling is the definitive mechanism underlying neuropathic pain. *Pain* **158** (Suppl 1):S55–S65.
Ueda H and Neyama H (2017) LPA1 receptor involvement in fibromyalgia-like pain induced by intermittent psychological stress, empathy. *Neurobiol Pain* **1**:16–25.
Ueda H, Neyama H, Nagai J, Matsushita Y, Tsukahara T, and Tsukahara R (2018a) Involvement of lysophosphatidic acid-induced astrocyte activation underlying the maintenance of partial sciatic nerve injury-induced neuropathic pain. *Pain* **159**: 2170–2178.
Ueda H, Neyama H, Sasaki K, Miyama C, and Iwamoto R (2018b) Lysophosphatidic acid LPA_1 and LPA_3 receptors play roles in the maintenance of late tissue plasminogen activator-induced central poststroke pain in mice. *Neurobiol Pain* **5**: 100020.
Welsch P, Üçeyler N, Klose P, Walitt B, and Häuser W (2018) Serotonin and noradrenaline reuptake inhibitors (SNRIs) for fibromyalgia. *Cochrane Database Syst Rev* **2**:CD010292.
Yokoyama T, Maeda Y, Audette KM, and Sluka KA (2007) Pregabalin reduces muscle and cutaneous hyperalgesia in two models of chronic muscle pain in rats. *J Pain* **8**: 422–429.
Zimmermann M (1983) Ethical guidelines for investigations of experimental pain in conscious animals. *Pain* **16**:109–110.

Address correspondence to: Hiroshi Ueda, Department of Molecular Pharmacology, Kyoto University Graduate School of Pharmaceutical Sciences, Yoshida Shimoadachi-cho, Sakyo-ku, Kyoto 606-8501, Japan. E-mail: ueda.hiroshi.8e@kyoto-u.ac.jp

The Journal of Pharmacology and Experimental Therapeutics

Mirtazapine, an α2 antagonist-type antidepressant reverses pain and lack of morphine analgesia in fibromyalgia-like mouse models

Hiroyuki Neyama[1], Naoki Dozono[2], Hitoshi Uchida[3], and Hiroshi Ueda[2]

Department of Pharmacology and Therapeutic Innovation, Nagasaki University Graduate School of Biomedical Sciences, Nagasaki, Japan

Supplementary Figures

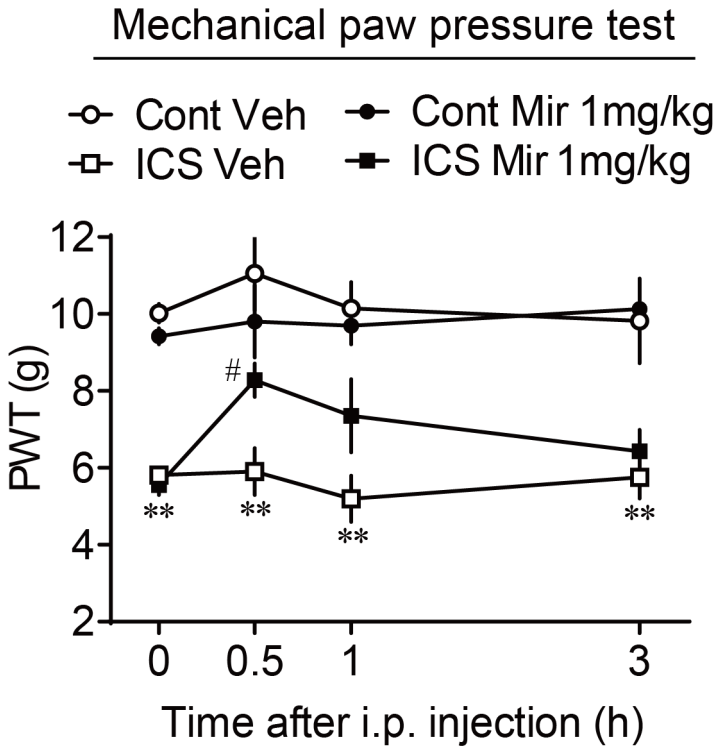

Supplementary Fig. 1.

Blockade of ICS-induced mechanical hyperalgesia by mirtazapine (Mir). Results represent the mechanical threshold (g) at indicated time points after vehicle (Veh) or Mir administration at the time point of P5 in control (Cont) and ICS-mice. Mir was administered at 1 mg/kg, i.p. **P<0.01, vs. Cont Veh, #P<0.05, vs. ICS Veh, two-way ANOVA followed by Tukey's multiple comparisons test (Interaction $F_{9, 48}$ = 0.8921, P=0.5394; Time: $F_{3, 48}$ = 1.931, P=0.1371, Treatment: $F_{3, 48}$ = 48.84, P<0.0001, n=4).

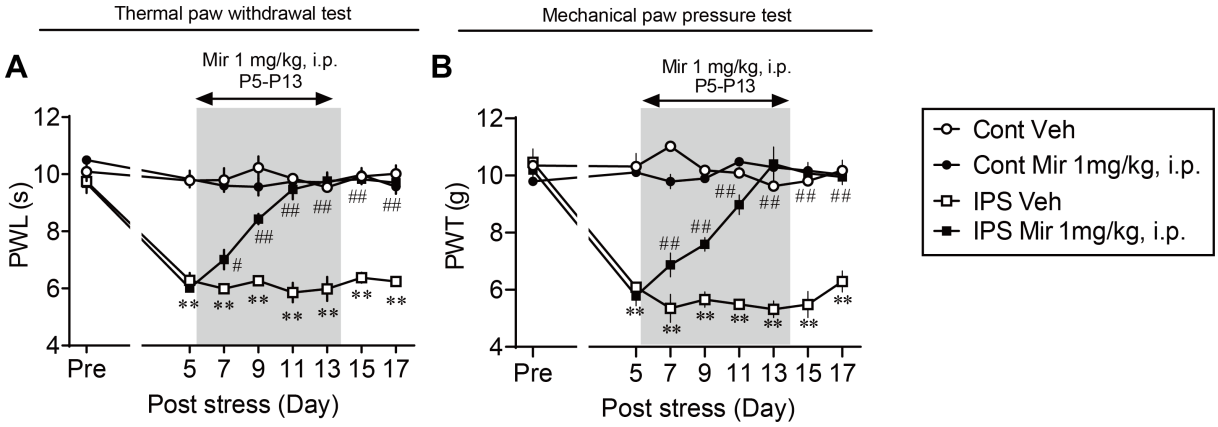

Supplementary Fig. 2

Long-lasting reversal of hyperalgesia following repeated treatments with mirtazapine in the IPS model. (A, B) Chronological change of basal thermal (**A**) or mechanical **(B)** paw withdrawal threshold after the IPS. Results represent the paw withdrawal latency (s) in **(A)**, and paw withdrawal threshold (g) in **(B)**. Nociceptive tests were performed prior to each Mir administration (P5, 7, 9 and 11), and at P13, 15 and 17. **p<0.01, vs. Cont Veh, ##p<0.01, #p<0.05, vs. IPS Veh, two-way ANOVA followed by Tukey's multiple comparisons test (**A**: Interaction $F_{21, 96}$=11.52, P<0.0001, Time $F_{7, 96}$=22.16, P<0.0001, Treatment $F_{3, 96}$=271.8, P<0.0001, n=4; **B**: Interaction $F_{21, 96}$=14.52, P<0.0001, Time $F_{7, 96}$=17.03, P<0.0001, Treatment

$F_{3, 96}$=254.7, P<0.0001, n=4).

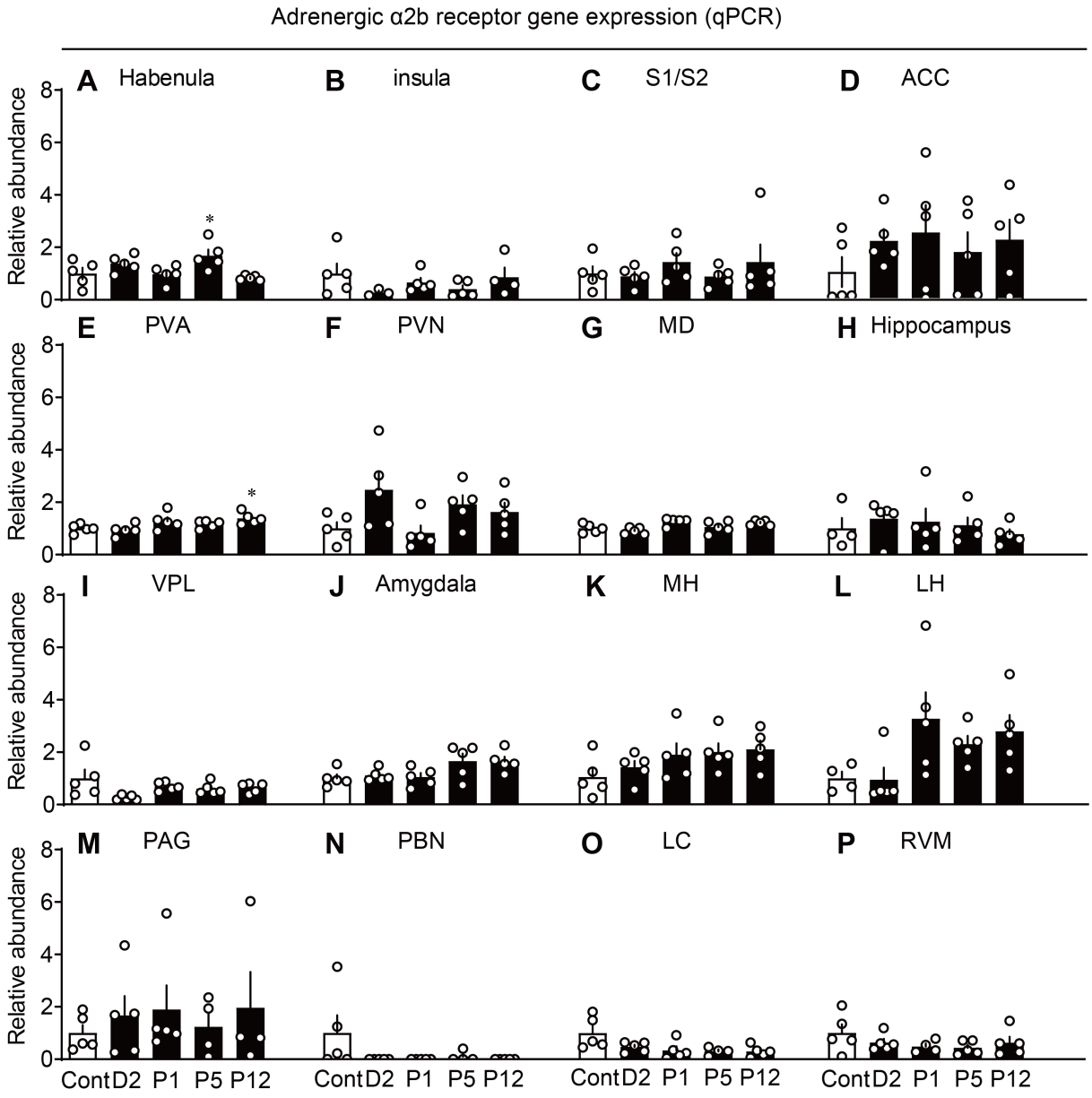

Supplementary Fig. 3

Lack of the alteration in adrenergic α2b receptor gene expression after ICS exposure (A-P) Time-course of adrenergic α2b receptor mRNA expression in the brain regions, including Habenula **(A)**, Insula **(B)**, S1 and S2 cortices **(C)**, ACC **(D)**, PVA **(E)**, PVN **(F)**, MD **(G)**,

Hippocampus **(H)**, VPL **(I)**, Amygdala **(J)**, MH **(K)**, LH **(L)**, PAG **(M)**, PBN **(N)**, LC **(O)**, RVM **(P)** after ICS exposure. The mRNA level of adrenergic α2b receptor was quantified by using qPCR and normalized to that of housekeeping gene GAPDH. Data are presented as percentage of each control day and expressed as the means ± S.E.M. from at least 3 mice. **(A, E)** *p<0.05, vs. Cont, one-way ANOVA followed by Dunnett's multiple comparisons test (**A**: $F_{4, 20}$=4.110, P=0.0137; **E**: $F_{4, 20}$=3.461, P=0.0264).

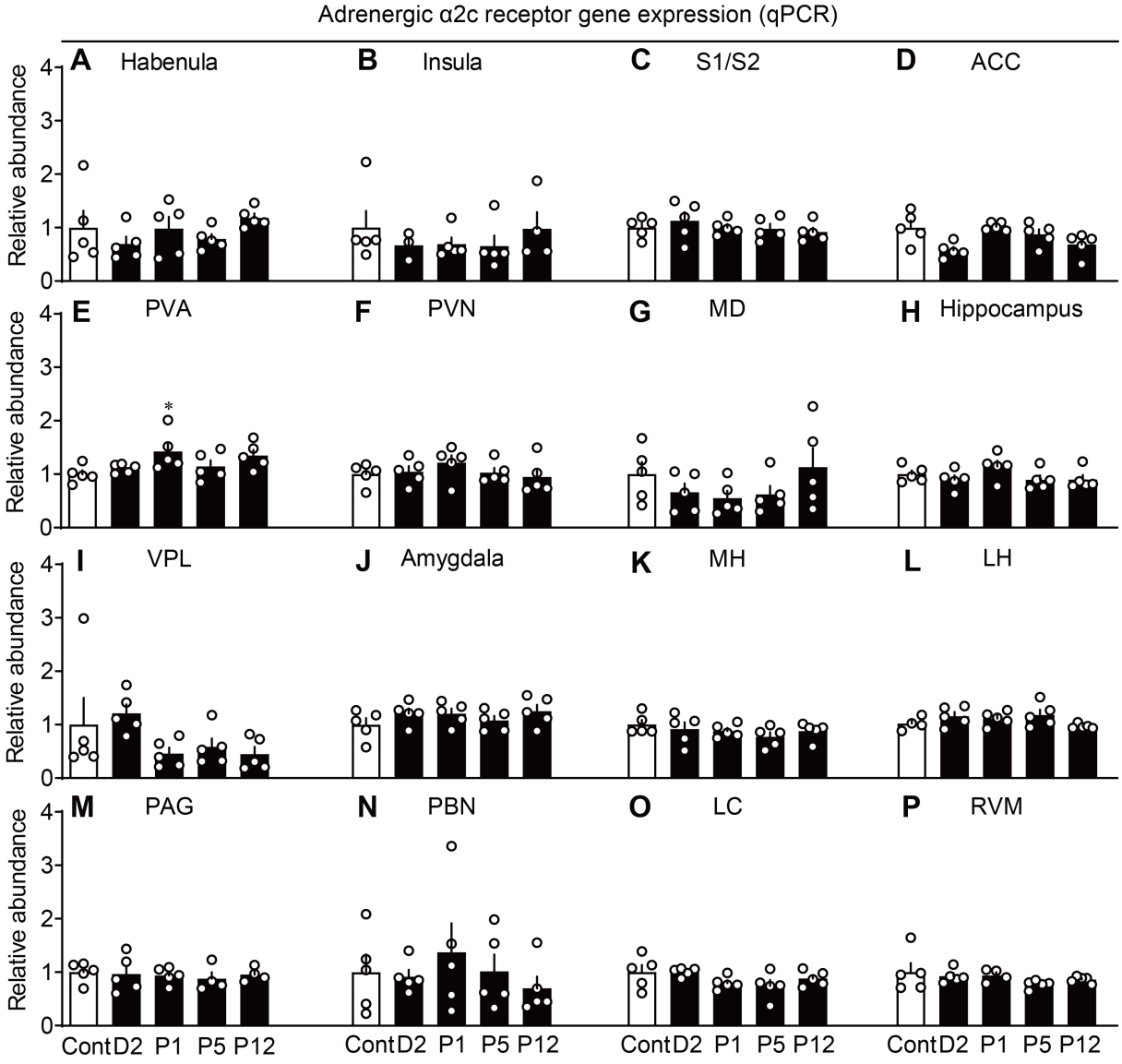

Supplementary Fig. 4

Lack of the alteration in adrenergic α2c receptor gene expression after ICS exposure (A-P) Time-course of adrenergic α2c receptor mRNA expression in the brain regions, including Habenula **(A)**, Insula **(B)**, S1 and S2 cortices **(C)**, ACC **(D)**, PVA **(E)**, PVN **(F)**, MD **(G)**, Hippocampus **(H)**, VPL **(I)**, Amygdala **(J)**, MH **(K)**, LH **(L)**, PAG **(M)**, PBN **(N)**, LC **(O)**, RVM **(P)** after ICS exposure. The mRNA level of adrenergic α2c receptor was quantified by using qPCR and normalized to that of housekeeping gene GAPDH. Data are presented as percentage of each control day and expressed as the means ± S.E.M. from at least 3 mice. **(E)** *$p<0.05$, vs. Cont, one-way ANOVA followed by Dunnett's multiple comparisons test ($F_{4, 20}=2.659$, $P=0.0629$).

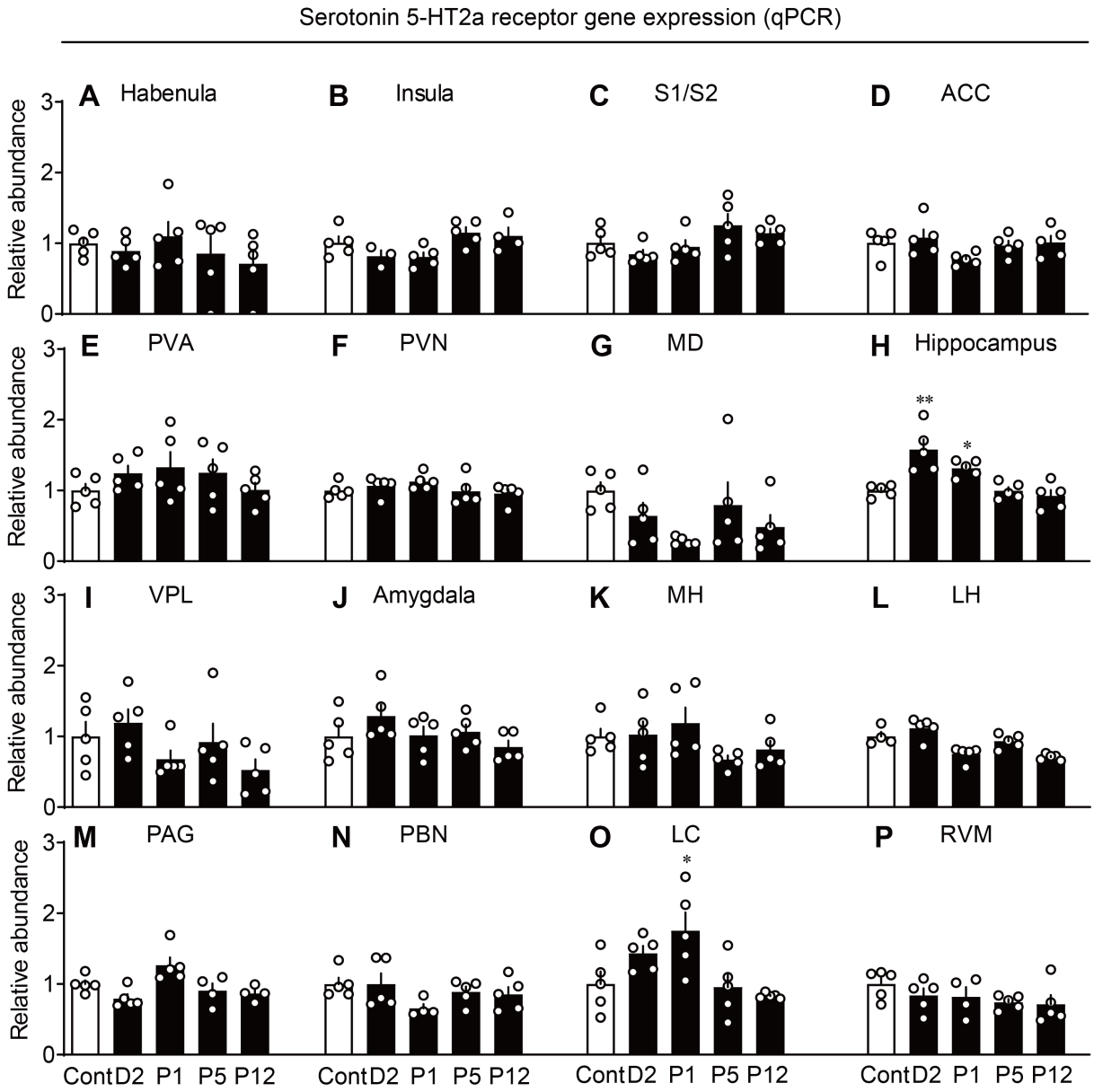

Supplementary Fig. 5

Lack of the alteration in serotonin 5-HT2a receptor gene expression after ICS exposure

(A-P) Time-course of serotonin 5-HT2a receptor mRNA expression in the brain regions, including Habenula **(A)**, Insula **(B)**, S1 and S2 cortices **(C)**, ACC **(D)**, PVA **(E)**, PVN **(F)**, MD **(G)**, Hippocampus **(H)**, VPL **(I)**, Amygdala **(J)**, MH **(K)**, LH **(L)**, PAG **(M)**, PBN **(N)**, LC **(O)**, RVM **(P)** after ICS exposure. The mRNA level of serotonin 5-HT2a receptor was quantified by using qPCR and normalized to that of housekeeping gene GAPDH. Data are presented as percentage of each control day and expressed as the means ± S.E.M. from at least 3 mice. **(H,**

O) **p<0.01, *p<0.05, vs. Cont, one-way ANOVA followed by Dunnett's multiple comparisons test (**H**: F4, 20 = 11.15, P<0.0001; **O**: $F_{4, 20}$ = 5.199, P=0.0049).

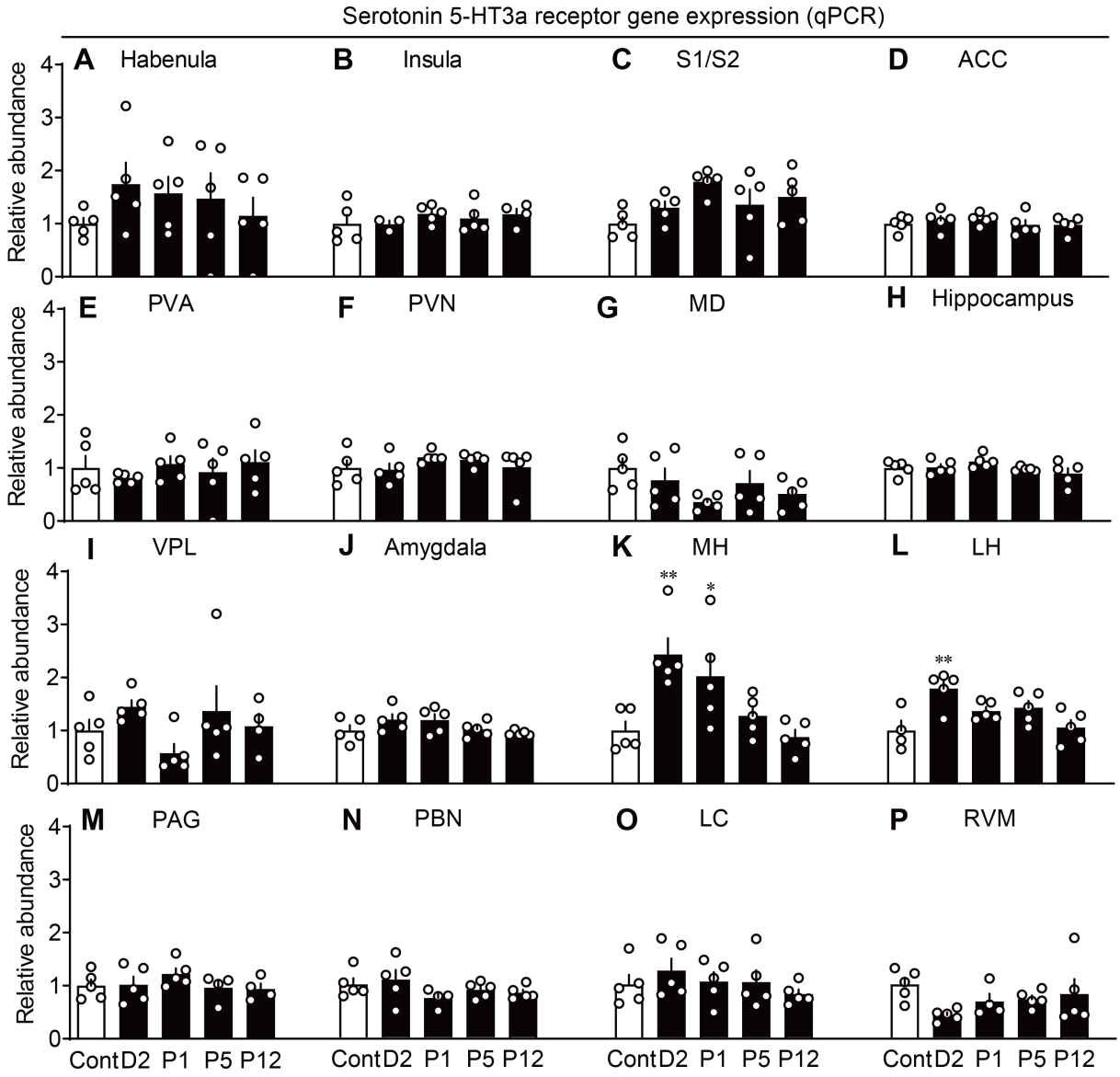

Supplementary Fig. 6

Lack of the alteration in serotonin 5-HT3a receptor gene expression after ICS exposure

(A-P) Time-course of serotonin 5-HT3a receptor mRNA expression in the brain regions, including Habenula **(A)**, Insula **(B)**, S1 and S2 cortices **(C)**, ACC **(D)**, PVA **(E)**, PVN **(F)**, MD **(G)**, Hippocampus **(H)**, VPL **(I)**, Amygdala **(J)**, MH **(K)**, LH **(L)**, PAG **(M)**, PBN **(N)**, LC **(O)**,

RVM **(P)** after ICS exposure. The mRNA level of serotonin 5-HT3a receptor was quantified by using qPCR and normalized to that of housekeeping gene GAPDH. Data are presented as percentage of each control day and expressed as the means ± S.E.M. from at least 3 mice. **(K, L)** **p<0.01, *p<0.05, vs. Cont, one-way ANOVA followed by Dunnett's multiple comparisons test (**K**: $F_{4, 20}$=6.562, P=0.0015; **L**: $F_{4, 19}$=5.311, P=0.0048).

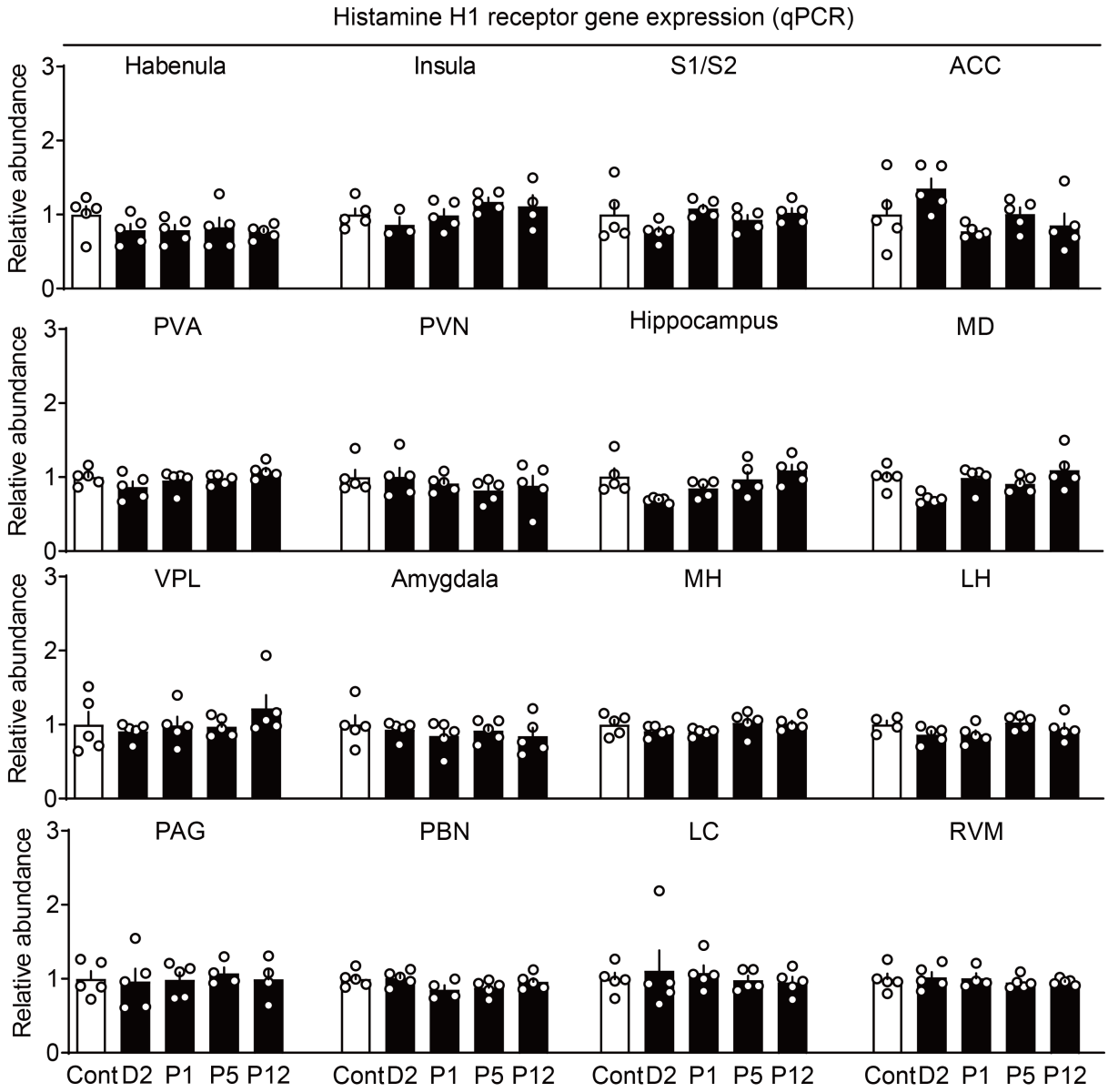

Supplementary Fig. 7

Lack of the alteration in histamine H1 receptor gene expression after ICS exposure (A-P)

Time-course of histamine H1 receptor mRNA expression in the brain regions, including Habenula **(A)**, Insula **(B)**, S1 and S2 cortices **(C)**, ACC **(D)**, PVA **(E)**, PVN **(F)**, MD **(G)**, Hippocampus **(H)**, VPL **(I)**, Amygdala **(J)**, MH **(K)**, LH **(L)**, PAG **(M)**, PBN **(N)**, LC **(O)**, RVM **(P)** after ICS exposure. The mRNA level of histamine H1 receptor was quantified by using qPCR and normalized to that of housekeeping gene GAPDH. Data are presented as percentage of each control day and expressed as the means ± S.E.M. from at least 3 mice.

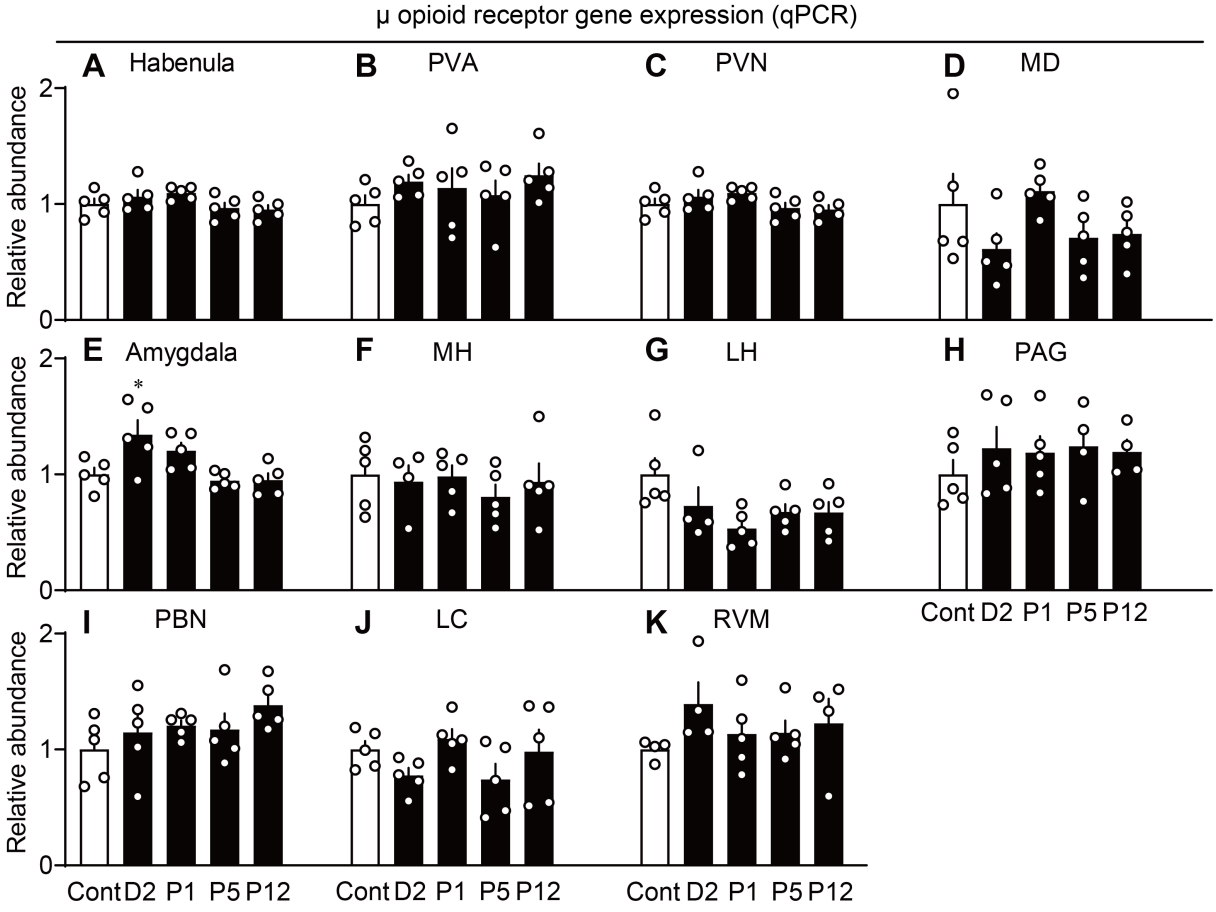

Supplementary Fig. 8.

Lack of the alteration in μ opioid receptor (MOPr) gene expression after ICS exposure (A-P) Time-course of MOPr mRNA expression in the brain regions, including Habenula **(A)**, Insula **(B)**, S1 and S2 cortices **(C)**, ACC **(D)**, PVA **(E)**, PVN **(F)**, MD **(G)**, Hippocampus **(H)**, VPL **(I)**, Amygdala **(J)**, MH **(K)**, LH **(L)**, PAG **(M)**, PBN **(N)**, LC **(O)**, RVM **(P)** after ICS exposure. The mRNA level of MOPr was quantified by using qPCR and normalized to that of housekeeping gene GAPDH. Data are presented as percentage of each control day and expressed as the means ± S.E.M. from at least 4 mice. **(E)** *$p<0.05$, vs. Cont, one-way ANOVA followed by Dunnett's multiple comparisons test ($F_{4, 20}=5.555$, $P=0.0036$).